Spectroscopic Study of B−Kr Nonbonding Interactions

Xin Yang and Paul J. Dagdigian*

Department of Chemistry, The Johns Hopkins University, Baltimore, Maryland 21218-2685

Received: January 29, 1997; In Final Form: March 17, 1997[⊗]

The fluorescence excitation spectrum of the BKr van der Waals complex in the vicinity of the B atomic $2s2p^2\ ^2D \leftarrow 2s^22p\ ^2P$ transition is reported. A vibrational progression in this spectrum is assigned to the $D^2\Pi \leftarrow X^2\Pi_{1/2}$ transition, in analogy with BAr. The lifetimes of BKr($D^2\Pi$) vibrational levels are considerably smaller than the B($2s2p^2\ ^2D$) atomic lifetime, indicative of an excited state predissociation. From the observed threshold for B($2s2p^2\ ^2D$) + Kr continuum excitation, we obtain estimates of the BKr dissociation energies for the ground $X^2\Pi_{1/2}$ ($D_0'' = 159.4 \pm 1.2$ cm^{-1}) and the excited $D^2\Pi$ ($D_0' = 120.6 \pm 1.2$ cm^{-1}) states. Two weak bands recorded in the same spectral region are tentatively assigned to the $E^2\Sigma^+ \leftarrow X^2\Pi_{1/2}$ transition. In the spectral region around the B atomic $2s^23s\ ^2S \leftarrow 2s^22p\ ^2P$ transition to the lowest Rydberg state, no bands assignable to diatomic BKr are found, in contrast to the BNe and BAr systems. Instead, complicated fluorescence excitation features are observed, and these are believed to be due to excitation of higher BKr_n clusters. It appears that both the $B^2\Sigma^+$ and $C^2\Delta$ states of BKr do not fluoresce because of predissociation through spin−orbit coupling to a repulsive quartet state.

1. Introduction

Spectroscopic studies of diatomic metal-rare gas van der Waals complexes can provide information on nonbonding interactions of these species.[1] These are essential ingredients for an understanding of the behavior of metal atoms in larger clusters and cryogenic matrices. Complexes involving the boron atom have been the focus of study in our laboratory. We have observed fluorescence excitation (FE) and depletion (FD) spectra of BNe[2, 3] and BAr,[4−7] as well as B···H_2[8, 9] and BAr_2.[10] With collaborative theoretical work by Alexander, Yarkony, and coworkers,[2,4,5,10−14] it has been possible to characterize the potential energy curves of several electronic states of these complexes, as summarized in a recent review.[15]

There are two resonance transitions in the boron atom for wavelengths longer than 200 nm, namely, $2s^23s\ ^2S \leftarrow 2s^22p\ ^2P$ at 249.8 nm and $2s2p^2\ ^2D \leftarrow 2s^22p\ ^2P$ at 208.9 nm.[16] The BRg (Rg = rare gas) molecular electronic states emanating from these excited asymptotes are denoted $B^2\Sigma^+$ for B($2s^23s\ ^2S$) + Rg and $C^2\Delta$, $D^2\Pi$, and $E^2\Sigma^+$ for B($2s2p^2\ ^2D$) + Rg. The potential energy curves of the $B^2\Sigma^+$ states of BNe and BAr were found to be dramatically different. The BAr($B^2\Sigma^+$) state possesses a deep inner well ($D_0' \approx 1000$ cm^{-1}) and a shallow outer well, separated by an intervening barrier approximately 108 cm^{-1} high.[10] By contrast, the BNe($B^2\Sigma^+$) state is purely repulsive, with only a slight inflection on the repulsive wall suggestive of a weak attraction.[2]

The sharp differences in BNe and BAr potential energy curves are also seen for the $C^2\Delta$ state. The binding energy of BNe($C^2\Delta$) ($D_0' = 111$ cm^{-1}) is slightly greater than that of the ground $X^2\Pi$ state.[2] This increase was rationalized as arising from reduced B−Ne repulsion upon $2p\pi \leftarrow 2s\sigma$ electronic excitation corresponding to the C ← X transition. In contrast to the modest binding of BNe($C^2\Delta$), the BAr($C^2\Delta$) binding energy is extremely large for a metal-argon van der Waals complex ($D_0' \approx 3540$ cm^{-1}).[7] Sohlberg and Yarkony[13] have investigated the binding in this state through electronic structure calculations. They find that the strong binding is the result of dative bonding through donation of electron density from the Ar $3p\sigma$ orbital to the empty B $2p\sigma$ orbital.

In contrast to the emitting BNe($C^2\Delta$) state, BAr($C^2\Delta$) decays nonradiatively and was detected only through fluorescence depletion spectroscopy.[7] In this technique,[9,17,18] a spectroscopic transition is observed by monitoring the effect of the so-called depletion laser on fluorescence induced by the probe laser. The nonradiative decay of BAr($C^2\Delta$) occurs by spin−orbit-induced predissociation through the repulsive $^4\Pi$ state correlating with the lower B($2s2p^2\ ^4P$) + Ar asymptote, which lies ∼19 000 cm^{-1} below B($2s2p^2\ ^2D$) + Ar.[14] We also found that the BAr($D^2\Pi$) state undergoes a weak predissociation. A clear identification of the perturbing state could not be made in this case.

In view of these dramatic differences in the BNe and BAr excited states, we have extended our study of BRg complexes to BKr. These experiments on BKr are reported in the present paper. We again find significant differences between the excited electronic states of BKr and those of the lighter BRg complexes. In particular, we conclude that the BKr($B^2\Sigma^+$) state decays nonradiatively, in contrast to the purely radiative decay of the bound BAr($B^2\Sigma^+$) vibrational states.[4] We also find that the BKr($D^2\Pi$) state is somewhat more strongly predissociated than BAr($D^2\Pi$). To our knowledge, the only all-electron quantum chemistry calculation of BKr potential energy curves was a complete active space self-consistent-field (CASSCF) calculation.[19] This study did not recover any of the weak binding of BKr electronic states since dispersion interactions were not included.

2. Experimental Section

Our experimental apparatus and procedures for obtaining FE and FD spectra and measuring excited state decay lifetimes have been described in detail previously.[2−4,7,9] High-pressure premixed gas samples of B_2H_6/Kr/Ne/He or B_2H_6/Kr/Ar/He (typically 6 atm, including 0.2% diborane and 25% Kr) were expanded supersonically into a vacuum chamber through a pulsed solenoid valve (0.2 cm diameter orifice). Boron atoms were generated through 193 nm photolysis of diborane at the nozzle orifice, and the BKr complex was detected 1.2 cm downstream of the nozzle by FE with a frequency-doubled dye laser. In FD experiments, another frequency-doubled dye laser beam overlapped the first one and was fired earlier, as described previously.[7,9]

[⊗] Abstract published in *Advance ACS Abstracts,* May 1, 1997.

S1089-5639(97)00349-6 CCC: $14.00 © 1997 American Chemical Society

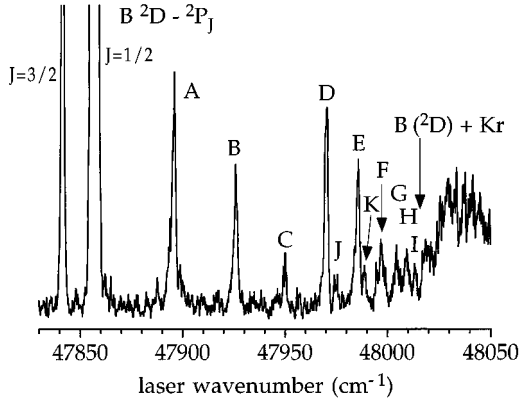

Figure 1. Low-resolution FE spectrum of a free jet containing boron atoms, produced by 193 nm photolysis of diborane, in a Kr(25%)/Ne/He mixture at a total backing pressure of 6 atm. The boron $2s2p^2\ ^2D_J \leftarrow 2s^22p\ ^2P_{1/2,3/2}$ atomic transitions are identified. Also observable in the spectrum are bands assigned to electronic transitions in the BKr complex (denoted as A−K). In addition, a continuous excitation is observed to the blue of 48 016.5 cm^{-1} (indicated with a vertical arrow in the figure). As discussed in the text, bands A−I are assigned as the (v',0) progression of the BKr $D^2\Pi-X^2\Pi_{1/2}$ electronic transition, with $v' = 0-8$, while bands J and K are tentatively assigned to the $E^2\Sigma^+-X^2\Pi_{1/2}$ (0,0) and (1,0) bands.

The laser-induced fluorescence signal passed through a $^1/_4$ m monochromator and was detected with a photomultiplier (EMI 9813QB), whose output was directed to a gated integrator and thence to a computer. A portion of the fundamental output of the dye laser was directed through a solid fused silica etalon (free spectral range 1.18 cm^{-1} in the visible) in order to provide wavenumber markers. The B atomic transitions[16] were employed for absolute wavenumber calibration.

For the measurement of decay lifetimes of excited levels, the output of the photomultiplier was connected to a digital oscilloscope (LeCroy Model 9360), which was triggered by a photodiode observing the fundamental dye laser radiation. The decay wave forms were transferred to a computer through a GPIB interface for storage and later analysis.

3. Results

3.1. Spectral Region around the B ^{2}D ← ^{2}P Transition. Figure 1 presents a low-resolution survey FE spectrum in this spectral region for a supersonic beam of a photolyzed B_2H_6/Kr/Ne/He mixture. The two sharp off-scale lines are the $2s2p^2\ ^2D \leftarrow 2s^22p\ ^2P_{1/2,3/2}$ atomic transitions, the strongest of which is the transition from the ground $^2P_{1/2}$ spin−orbit level. The small spin−orbit splitting[16] of the excited ^{2}D level was not resolved. Essentially identical FE spectra were obtained with photolyzed B_2H_6/Kr/Ar/He mixtures.

Also observable in Figure 1 are a number of discrete molecular bands (denoted A−K), as well as unstructured excitation at higher wavenumbers. These features are assigned to the BKr complex for the following reasons. This spectrum was observed only when the source gas mixture was photolyzed and Kr was included in the mixture. The relative intensities of these features were found to be independent of the gas backing pressure and the Kr mole fraction, which was varied from 10 to 80%. This spectrum appears in the same wavenumber range as the B $2s2p^2\ ^2D \leftarrow 2s^22p\ ^2P$ atomic transition and, moreover, closely resembles the corresponding BAr FE spectrum.[7] When Kr was removed from the seed gas mixture, the molecular features displayed in Figure 1 disappeared, and the spectrum of BNe or BAr appeared instead. This behavior can be rationalized by the different BRg binding energies. FE scans were taken over the wavenumber range 47 610−48 135 cm^{-1}. The only molecular features observed were those displayed in Figure 1.

The broad feature at the high wavenumber end of the spectrum shown in Figure 1 changed shape slightly as a function of the source backing pressure and the Kr mole fraction. Hence, it is possible that transitions in higher BKr_n clusters may be contributing to this feature. However, the onset, at 48 016.5 ± 1.0 cm^{-1}, was found to be invariant to source conditions. We hence assign this as the threshold for excitation from $BKr(X^2\Pi_{1/2},v''=0)$ to the $B(2s2p^2\ ^2D)$ + Kr continuum. The difference between this wavenumber and that for the B $2s2p^2\ ^2D \leftarrow 2s^22p\ ^2P_{1/2}$ atomic transition[16] provides an estimate of the dissociation energy of the ground $X^2\Pi_{1/2}$ state, $D_0'' = 159.4 \pm 1.2$ cm^{-1}. As discussed previously for BNe and BAr,[3,4,7] this value is, strictly speaking, an upper limit since there could be a barrier to dissociation. However, we believe that there should be no barriers in the potential energy curves of molecular states correlating with the $B(2s2p^2\ ^2D)$ + Rg asymptote.

Bands A−I appear to form a (v',0) vibrational progression, in analogy with the corresponding BAr bands seen in this spectral range. We assign band A as excitation to $v' = 0$ since it is the strongest band in this progression, and no other bands were found at lower wavenumbers. Accordingly, the excited state dissociation energy ($D_0' = 120.6 \pm 1.2$ cm^{-1}) was estimated from the wavenumber difference between band A and the assigned threshold for the $B(2s2p^2\ ^2D)$ + Kr continuum. Bands B−I appear to be higher members of this progression. These bands are found to be all red degraded. This suggests that the average B−Kr internuclear separations in the excited vibrational levels are greater than in the ground $v'' = 0$ vibrational level, consistent with the observed decrease in the binding energy upon electronic excitation. We assign bands A−I to the BKr $D^2\Pi \leftarrow X^2\Pi_{1/2}$ transition, from analogy with the spectrum of BAr.[7] The $D^2\Pi$ state is expected to have a binding energy slightly less than that of the $X^2\Pi_{1/2}$ state.

For several reasons, we did not attempt to record high-resolution scans of these bands in order to resolve their rotational structure. We were able to achieve only partial rotational resolution for the corresponding BAr bands.[7] The signal-to-noise ratios in our FE spectra for BKr were poorer than those recorded previously[7] for BAr. This is due, in part, to an increased excited state predissociation in the former complex, and hence a reduced fluorescence quantum yield, as we describe in more detail below. In addition, we expect considerable overlapping of the rotational lines of the BKr isotopomers, since both B and Kr have several naturally occurring isotopes[20] [boron: ^{11}B, 80.22%; ^{10}B, 19.78%. krypton (abundance >10%): ^{84}Kr, 56.90%; ^{86}Kr, 17.37%; ^{82}Kr, 11.55%; ^{83}Kr, 11.56%]. The isotope shifts of the bands will be dominated by the reduced mass change upon B isotopic substitution. Based on the vibrational constants presented below, the ^{11,10}BKr isotope splittings are calculated to be ≤1.7 cm^{-1} and would be difficult to observe in our FE spectra.

Table 1 presents transition wavenumbers for the D−X (v',0) bands. These were determined as the wavenumber corresponding to the maximum intensity in each band. Since the rotational temperature in these beams were quite cold (2 K in case of BAr[7]), these should be reasonably close to the band origin wavenumbers. Molecular orbital arguments[3] suggest that the spin−orbit splitting in the $D^2\Pi$ state should be small, as inferred for BAr.[7]

We expect a smooth variation in the intensity of bands within a (v',0) progression. Hence, the low relative intensity of several of the bands in Figure 1 ($v' = 1$, band B; $v' = 2$, band C) is

TABLE 1: Transition Wavenumbers for the BKr $D^2\Pi$, $E^2\Sigma^+ - X^2\Pi_{1/2}$ (v′,0) Bands Observed by FE Spectroscopy

band ID	v'	$T_{v'}$ [a]	O−C[b]
	$D^2\Pi - X^2\Pi_{1/2}$ Transition		
A	0	47 895.9	+0.1
B	1	47 926.3	+0.0
C	2	47 950.6	−0.5
D	3	47 970.8	+0.1
E	4	47 986.2	+0.4
F	5	47 997.2	+0.2
G	6	48 004.5	−0.4
H	7	48 010.0	−0.2
I	8	48 013.8	+0.2
	$E^2\Sigma^+ - X^2\Pi_{1/2}$ Transition[c]		
J	0?	47 975.0 ± 1.2	
K	1?	47 989.2 ± 0.8	

[a] Unless otherwise noted, estimated uncertainties ±0.5 cm^{-1}. [b] Difference between observed and calculated wavenumbers, using the vibrational parameters reported in the text. [c] Vibrational assignment uncertain. See text.

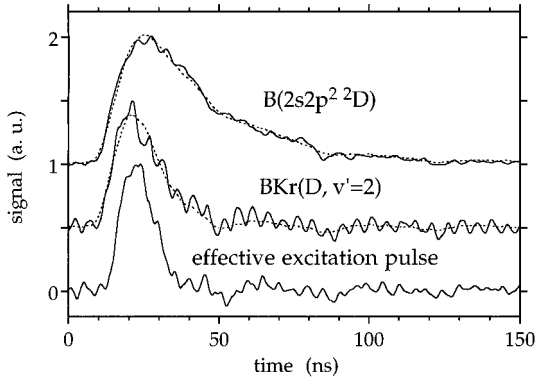

Figure 2. Fluorescence decay waveforms for excitation of the B($2s2p^2$ ^{2}D) atomic level and the BKr($D^2\Pi$,v'=2) vibrational level. The solid and dotted lines denote the experimental and fitted profiles, respectively. The effective excitation pulse, obtained as described in the text, is also plotted. All profiles are normalized to unit amplitude and displaced vertically for clarity.

puzzling. A similar irregular pattern of intensities was previously found in the BAr D−X (v',0) progression and was ascribed to a vibrational state-dependent predissociation, on the basis of measured excited state decay lifetimes.[7] In order to see whether a similar nonradiative decay process is affecting the BKr(D,v') levels, we have measured decay lifetimes for the $v' = 0-4$ levels.

Decay profiles were obtained by taking the difference between waveforms acquired with the excitation laser tuned on and off a molecular band. The lifetimes appeared to be comparable to or shorter than the laser pulse width (∼13 ns). Hence, they were determined by fits to a model profile consisting of a convolution of the measured laser pulse shape with an exponential decay. The effective excitation pulse, namely, the convolution of the actual laser pulse with the temporal response of the detection system, was determined at the same photomultiplier voltage used during the acquisition of the BKr decay profiles by recording the Rayleigh scattered light signal with low-pressure air in the apparatus and is displayed in the lower panel of Figure 2. A fast iterative technique[21] for the convolution of the effective laser pulse with the exponential decay and the Levenberg−Marquardt algorithm[22] for nonlinear least-squares fitting was employed for the determination of the decay rates. As described previously,[7] this procedure for the determination of decay lifetimes was validated by good agreement of our measured lifetime (24.3 ± 2.4 ns) for the B($2s2p^2$ ^{2}D) atomic level with the most recent literature value[23] (23.1 ± 1.2 ns). Our measured and fitted decay profiles for this atomic level are shown in Figure 2.

TABLE 2: Measured Decay Lifetimes for BKr($D^2\Pi$) Vibrational Levels

band excited	excited level	decay lifetime (ns)[a]	band excited	excited level	decay lifetime (ns)[a]
A	$v' = 0$	11.0	D	$v' = 3$	12.7
B	$v' = 1$	8.1	E	$v' = 4$	13.5
C	$v' = 2$	6.8			

[a] Estimated uncertainties ±1.2 ns.

In the absence of a nonradiative decay process, we expect the lifetimes of the BKr($D^2\Pi$) vibrational levels to be the same as that for the B($2s2p^2$ ^{2}D) level.[3,7] Figure 2 displays a fluorescence decay profile for the excited level with the shortest decay lifetime, BKr($D^2\Pi$, $v' = 2$). It can be seen that the decay lifetime is, in fact, considerably shorter than the atomic lifetime. Table 2 presents our measured lifetimes for vibrational levels $v' = 0-4$. All of these are significantly smaller than the atomic lifetime and the lifetimes of the BAr($D^2\Pi$) vibrational levels, reported previously.[7] Hence, we conclude that BKr($D^2\Pi$) is subject to a nonradiative decay process, which causes a reduction of the fluorescence quantum yield. Since the lifetime of $v' = 2$ is the smallest of those measured, this level will have the smallest fluorescence quantum yield, and hence the intensity of the (2,0) band should be significantly depressed, as observed. However, we do note that our measured decay lifetimes do not provide a completely quantitative explanation of the reduced band intensities. For example, the lifetimes of $v' = 2$ and 3 presented in Table 2 suggest that the fluorescence quantum yields for the (2,0) and (3,0) bands (features C and D in Figure 1) differ by a factor of 2; however, the difference in the observed intensities of these bands is greater than that. We note that the fractional uncertainties in our measured lifetimes are large because the lifetimes are short. It is nevertheless clear that BKr($D^2\Pi$) decays both radiatively and nonradiatively.

In order to provide estimates for the vibrational constants of the BKr($D^2\Pi$) state, we have carried out a fit of the transition wavenumbers $T_{v'}$ reported in Table 1 to a polynomial in powers of $(v' + {}^1/_2)$. A fit to a quadratic expression yielded deviations between measured and fitted wavenumbers greater than our estimated uncertainties. Instead, we employed a cubic expression and obtained the following parameters: $T_{e0} = 47\,878.1 \pm 0.4$, $\omega_e' = 36.97 \pm 0.42$, $\omega_e x_e' = 3.38 \pm 0.11$, $\omega_e y_e' = 0.106 \pm 0.008$ (all in cm^{-1}). The parameter T_{e0} is defined as the wavenumber separation between the minimum of the BKr($D^2\Pi$) potential energy curve and the BAr($X^2\Pi_{1/2}$,v''=0) level. It can be seen from the differences between measured and calculated wavenumbers reported in Table 1 that these parameters reproduce well the experimentally determined band positions.

Bands J and K (see Figure 1 and Table 1) do not appear to be part of the $D^2\Pi - X^2\Pi_{1/2}$ band system. The wavenumber differences from the adjacent bands D and E, respectively, are too large, on the basis of the above-reported vibrational constants, to be consistent with ^{11,10}BKr isotope splittings. Accordingly and in analogy with our observations on BAr,[7] we assign these to the $E^2\Sigma^+ \leftarrow X^2\Pi_{1/2}$ transition. In addition to these bands, we observe a very weak feature at lower wavenumbers between bands C and D at 47 956.5 ± 1.0 cm^{-1}, which could be another member of this band system. However, this feature was not observed with sufficiently high signal-to-noise ratio for a positive identification. Hence, we report in Table 1 only a tentative vibrational assignment for this band system. On this basis, we can only quote a lower limit to the binding energy of the BKr($E^2\Sigma^+$) state: $D_0' \geq 41.5 \pm 1.6$ cm^{-1}.

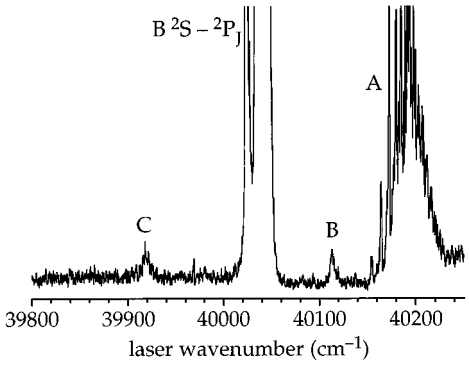

Figure 3. Low-resolution FE spectrum for a photolyzed B_2H_6/Kr/Ne/He beam in the spectral range of the B $2s^23s\ ^2S \leftarrow 2s^22p\ ^2P$ atomic transition. Features A−C are assigned to BKr_n clusters.

As in the case of BAr,[7] no bands assignable to the $C^2\Delta \leftarrow X^2\Pi$ transition were observed in FE scans. We believe that BKr($C^2\Delta$) decays nonradiatively, as does the corresponding state of BAr.

3.2. Spectral Region around the B $^2S \leftarrow ^2P$ Transition. We have also taken FE scans in the spectral region around the $2s^23s\ ^2S \leftarrow 2s^22p\ ^2P$ transition to the lowest atomic Rydberg level. Figure 3 displays such a scan. In addition to the strong B atomic lines, we observe three molecular features. Feature A has a complicated structure, which cannot be assigned to a transition to a bound (as in BAr[4]) or repulsive (as in BNe[2]) electronic state in a diatomic complex. Feature A appears at low Kr mole fraction, while features B and C become observable at higher mole fractions. We believe that the molecular carrier of these three features is higher BKr_n clusters, of different size.

We have carried out FD scans in order to verify that the carrier of feature A is different than that for the bands around the $^2D \leftarrow ^2P$ atomic line assigned to BKr. A probe laser was tuned to excite feature A, while a depletion laser (150 μJ pulse energy) was fired 150 ns before the probe laser and scanned through the BKr D−X (0,0) band. No depletion of the probe laser induced fluorescence was observed, as expected.

We also attempted to employ FD spectroscopy to observe the BKr $B^2\Sigma^+-X^2\Pi_{1/2}$ bands. While the corresponding BAr bands are observable by FE excitation,[4] we have also been able to detect these bands by FD spectroscopy, in which the BAr D−X (0,0) band was employed as the probe transition. The maximum depletion (70%) was observed upon excitation of the BAr B−X (8,0) band, with 80 μJ depletion laser pulse energy. In an analogous fashion, we searched for the BKr B−X band system while detecting BKr by FE through its D−X (0,0) band. Unfortunately, our sensitivity to small depletions was poor because the FE intensity of the BKr probe transition was much smaller than for BAr, and no BKr B − X bands were found. As discussed previously, there are a number of BKr isotopomers, and the peak intensities for a BKr band will be reduced by the significant isotopomeric splittings for an expected deeply bound BKr($B^2\Sigma^+$) state.

We believe that the BKr B−X transition was not observed in the FE scans since the excited $B^2\Sigma^+$ state decays nonradiatively. While it is usually difficult to argue on the basis of the lack of observation of a signal, our observation of the BKr D−X transition shows that we do indeed generate the BKr complex in these supersonic expansions. While it is possible, in principle, that we have not detected the BKr B−X transition because of poor Franck−Condon overlap, we were able to detect this transition in both BAr and BNe, despite very different shapes of the excited state potential energy curves. The Franck−Condon region in BAr($B^2\Sigma^+$) lies on the outer limb, just inside a barrier.[4] By contrast, the BNe($B^2\Sigma^+$) potential energy curve is purely repulsive.[2] We discuss the mechanism of nonradiative decay in the next section.

TABLE 3: Dissociation Energies for Several ^{11}BRg Electronic States

electronic state	BNe[a]	BAr[b]	BKr[c]
$X^2\Pi$	21	102	159
$D^2\Pi$	8	63	121

[a] Reference 2. [b] Reference 7. [c] This work.

4. Discussion

We find that the BKr binding energies for the $X^2\Pi$ and $D^2\Pi$ states are somewhat larger than those for the corresponding BNe and BAr states, as can be seen from the data in Table 3. As has been observed for many other metal−rare gas complexes,[1] the binding energies increase with increasing rare gas atomic number. We can rationalize the decreased binding energies of the $D^2\Pi$ states as compared to those of the corresponding ground $X^2\Pi$ states by consideration of the electron repulsion with different orbital occupancies on the B atom. The $X^2\Pi$ and $D^2\Pi$ states can be described by the electron configurations $2s\sigma^22p\pi$ and $2s\sigma2p\sigma2p\pi$, respectively. This $2p\sigma \leftarrow 2s\sigma$ excitation would be expected to decrease the binding energy of the complex slightly because of the more directional character of the $2p\sigma$ orbital along the internuclear axis.

We have found that the decay lifetimes of $D^2\Pi$ vibrational levels are more than a factor of 2 smaller than for the corresponding atomic state, B($2s2p^2\ ^2D$). A somewhat smaller reduction of decay lifetimes was found for BAr($D^2\Pi$) vibrational levels.[7] This electronic state must be decaying nonradiatively through a predissociation process. As discussed previously,[7] this cannot be caused by direct coupling with a repulsive state emanating from a lower energy asymptote since we have already accounted for all such states. The most likely mechanism is an indirect predissociation[24] through the $^2\Pi$ or $^2\Sigma^+$ state emanating from the B($2s^23p\ ^2P$) + Rg asymptote, which lies only 755 cm^{-1} above B($2s2p^2\ ^2D$) + Rg.[16] The enhanced nonradiative decay rates for BKr vs BAr are due to an enhanced nonadiabatic coupling in the former.

As in the BAr complex,[7] we could not detect the BKr($C^2\Delta$) state by FE. We expect that this state is also predissociated by the repulsive $^4\Pi$ state correlating with the B($2s2p^2\ ^4P$) + Kr asymptote. The BKr($C^2\Delta$) binding energy is probably greater than the already substantial binding energy of the BAr($C^2\Delta$) energy.

The observations presented in this paper strongly suggest that the BKr($B^2\Sigma^+$) state is predissociated. The most likely cause of predissociation is spin−orbit coupling to the repulsive $^4\Pi$ state, which crosses both the $B^2\Sigma^+$ and $C^2\Delta$ states. In the case of BAr, the $B^2\Sigma^+$ state decays radiatively, and there is no evidence that it is significantly predissociated.[4] The one-electron part of the $B^2\Sigma^+-{}^4\Pi$ spin−orbit matrix element is zero, assuming that the boron orbitals are not significantly perturbed by the approach of the Ar atom. The weak two-electron portion of the spin−orbit matrix element is probably too small to compete with the fast radiative decay of the $B^2\Sigma^+$ state. (The radiative lifetime of the corresponding B($2s^23s\ ^2S$) state is 4 ns.[23]) By contrast, Kr is much heavier than Ar, and apparently spin−orbit-induced predissociation in BKr competes effectively with radiative decay through the heavy atom effect.

Acknowledgment. This research was supported by the U.S. Air Force Office of Scientific Research under Grant F49620-95-1-0055. We gratefully acknowledge numerous conversations

with and the encouragement of Millard Alexander. We also thank David Yarkony and Karl Sohlberg for carrying out a computational study of predissociation of the BAr($C^2\Delta$) state. Their work helped provide us with insight to interpret the present experimental results.

References and Notes

(1) Breckenridge, W. H.; Jouvet, C.; Soep, B. In *Advances in Metal and Semiconductor Clusters*; Duncan, M. A., Ed.; JAI Press: Greenwich, 1995; p 1.
(2) Yang, X.; Hwang, E.; Dagdigian, P. J.; Yang, M.; Alexander, M. H. *J. Chem. Phys.* **1995**, *103*, 2779.
(3) Yang, X.; Hwang, E.; Dagdigian, P. J. *J. Chem. Phys.* **1996**, *104*, 599.
(4) Hwang, E.; Huang, Y.-L.; Dagdigian, P. J.; Alexander, M. H. *J. Chem. Phys.* **1993**, *98*, 8484.
(5) Hwang, E.; Dagdigian, P. J.; Alexander, M. H. *Can. J. Chem.* **1994**, *72*, 821.
(6) Hwang, E.; Dagdigian, P. J. *Chem. Phys. Lett.* **1995**, *233*, 483.
(7) Yang, X.; Dagdigian, P. *J. Chem. Phys.* **1997**, *106*, xxxx.
(8) Yang, X.; Hwang, E.; Alexander, M. H.; Dagdigian, P. J. *J. Chem. Phys.* **1995**, *103*, 7966.
(9) Yang, X.; Hwang, E.; Dagdigian, P. J. *J. Chem. Phys.* **1996**, *104*, 8165.
(10) Alexander, M. H.; Walton, A. R.; Yang, M.; Yang, X.; Hwang, E.; Dagdigian, P. J. *J. Chem. Phys.* **1997**, *106*, xxxx.
(11) Alexander, M. H. *J. Chem. Phys.* **1993**, *99*, 6014.
(12) Alexander, M. H.; Yang, M. *J. Chem. Phys.* **1995**, *103*, 7956.
(13) Sohlberg, K.; Yarkony, D. R. *J. Phys. Chem.* **1997**, *101*, xxxx.
(14) Sohlberg, K.; Yarkony, D. R. *J. Chem. Phys.* **1997**, *106*, xxxx.
(15) Dagdigian, P. J.; Yang, X.; Hwang, E. In *Highly Excited States: Relaxation, Reactions, and Structure*; Mullin, A. S., Schatz, G. C., Eds.; American Chemical Society, Washington, DC, 1997; p xxx.
(16) Odintzova, G. A.; Striganov, A. R. *J. Phys. Chem. Ref. Data* **1979**, *8*, 63.
(17) Loomis, R. A.; Schwartz, R. L.; Lester, M. I. *J. Chem. Phys.* **1996**, *104*, 6984.
(18) Basinger, W. H.; Lawrence, W. G.; Heaven, M. C. *J. Chem. Phys.* **1995**, *103*, 7218.
(19) Taylor, P. R. *Chem. Phys.* **1986**, *105*, 79.
(20) *American Institute of Physics Handbook*; McGraw-Hill: New York, 1972.
(21) Demas, J. N. *Excited State Lifetime Measurements*; Academic: New York, 1983.
(22) Press, W. H.; Flannnery, B. P.; Teukolsky, S. A.; Vetterling, W. T. *Numerical Recipes: The Art of Scientific Computing*; Cambridge University Press: New York, 1989.
(23) O'Brian, T. R.; Lawler, J. E. *Astron. Astrophys.* **1992**, *255*, 420.
(24) Lefebvre-Brion, H.; Field, R. W. *Perturbations in the Spectra of Diatomic Molecules*; Academic: New York, 1986.